Special Topic Article

3. Kinetic Computer Modeling of Microwave Surface-Wave Plasma Production

GANACHEV Ivan P.
Shibaura Mechatronics Corporation, Yokohama 247-8560, Japan
(Received 14 November 2003)

Abstract:
Kinetic computer plasma modeling occupies an intermediate position between the time consuming rigorous particle dynamic simulation and the fast but rather rough cold- or warm-plasma fluid models. The present paper reviews the kinetic modeling of microwave surface-wave discharges with accent on recent kinetic self-consistent models, where the external input parameters are reduced to the necessary minimum (frequency and intensity of the applied microwave field and pressure and geometry of the discharge vessel). The presentation is limited to low pressures, so that Boltzman equation is solved in non-local approximation and collisional electron heating is neglected. The numerical results reproduce correctly the bi-Maxwellian electron energy distribution functions observed experimentally.
Keywords:
surface-wave plasma, kinetic modeling, non-local approximation, electron plasma resonance, transit-time non-collisional electron heating

3.1 Microwave Surface-Wave Plasma

An electromagnetic wave propagating along the interface between two media with amplitude decaying exponentially away from the surface is referred to as "surface wave" (SW). A surface-wave plasma (SWP) is a discharge sustained by a surface wave propagating along the interface between an overdense plasma and a dielectric medium [1,2] without applying external static magnetic field. SW discharges [3-6] are increasingly being used for surface processing in the semiconductor and other industries (for reviews see [7-10]). The major advantages for their application are [10]: (a) easy operation at the moderate gas pressures (hundreds of Pa) required for high rates of isotropic processing, where inductively coupled, capacitively coupled and ECR plasmas fail, as well as at the low pressures (1 Pa and below) required for high aspect ratio anisotropic etching; (b) microwave field localization in the skin layer near the interface so that microwave induced damage at the processed surface (located deeper into the plasma volume) is avoided.

Let us outline the main features of microwave surface-wave plasmas important for their computer modeling. (A) At the industrially permissible excitation frequencies (typically 2.45 GHz) and required electron densities (typically 10^{11} cm^{-3}) the wavelengths and skin-depths are comparable or much shorter than the typical equipment size, which is not the case with the classical inductively or capacitively discharges operated usually at 13.56 MHz. Thus a uniform-amplitude approximation of the oscillating EM (electromagnetic) field becomes impossible. (B) The wave frequency ω is comparable to the electron plasma frequency ω_p in the entire plasma volume and even higher than it near the plasma boundary. Since ω_p^{-1} is the time scale for the sheath formation, this means that the sheath remains largely unchanged during one time period of the oscillating EM field. This is a major difference with conventional 13.56 MHz capacitively coupled plasmas, where the electron density and the sheath voltage follow the oscillations of the externally applied electric field. For modeling this means that one can consider the electron density and plasma potential as constant in time. Moreover, the field oscillation frequency ω is much higher than the inelastic collision frequency ν^* so that the explicit time dependence in the EEDF (electron energy distribution function) $f(\boldsymbol{v}, \boldsymbol{r}, t)$ is eliminated and kinetic models need to solve only the stationary Boltzmann kinetic equation

$$\boldsymbol{v}\cdot\nabla f + \frac{e}{m_e}\left(\tilde{\boldsymbol{E}} - \nabla\Phi\right)\cdot\nabla_{\boldsymbol{v}} f = S(f) + S^*(f) \qquad (1)$$

for the stationary EEDF $f(\boldsymbol{v}, \boldsymbol{r})$. In (1) S and S^* are the elastic and inelastic collision integrals, $\tilde{\boldsymbol{E}}$ is the oscillating part of the electric field, $\Phi(\boldsymbol{r})$ is the static plasma potential and $e = -|e| < 0$ and m_e are the electron charge and mass, respectively. An additional consequence of the non-moving sheaths is the absence of stochastic heating [11,12] in them.

author's e-mail: ivan.ganachev@shibaura.co.jp

(C) There is a new mechanism of transit-time non-collisional heating: Close to the plasma boundary there can be a surface where $\omega_p = \omega$. At this position an electron plasma resonance [13-16] occurs, resulting in even higher inhomogeneity of the oscillating field amplitude. Electrons flying through this resonance can experience transit-time heating [17] if the resonance is thin enough for them to pass through it much faster than the wave time period $2\pi/\omega$ (0.4 ns for $2\pi = 2.45$ GHz). For a typical 6 eV electron flying at 1.3×10^6 m/s this requires the resonance width to be of the order of 0.6 mm or less, a requirement which may be met or not depending on the specific conditions.

Below we review briefly the three major families of simulation methods. Due to space constrains only one is treated in more details, while for the other two we limit ourselves to some key ideas and references.

3.2 Direct Particle Dynamic Simulation

Direct particle dynamic simulation (PIC, PIC-MCC etc.) [18-20] provides the most rigorous and at the same time least developed approach to SWP modeling. PIC and PIC-MCC codes are attractive because they transfer the burden of making approximations and deciding what to take into account and what not to the computer. Still, there are not so many cases where PIC/PIC-MCC codes are indeed necessary (unless one really wants to put all the burden on the computer). In many cases one gets only a confirmation of results anyway expected from fluid or Boltzmann kinetic modeling.

A nice example of PIC-MCC simulation for SWP plasma is the analysis of local plasma resonance at $\omega_p = \omega$ in [21-23]. It demonstrates the non-collisional electron heating in the resonance resulting in non-Maxwellian EEDF with low-temperature bulk and high-temperature tail populations.

3.3 Fluid Models

Fluid models treat the plasma as a set of two fluids – electrons and ions – each one with its specific density, velocity and temperature, immersed in the microwave field. The EEDF is assumed known. There are different degrees of self-consistency: (a) simply solving for the fields while treating the plasma as an externally given medium [1,2,15,16,24-28]; (b) assuming some phenomenological (usually linear) relation between the absorbed microwave power and the plasma density [29-33]; (c) solving the particle balance including a phenomenological local relation between the microwave field and the ionization rate [34-37]; or (d) adding a degree of non-locality by including the electron heat flow (diffusion of hot electrons from the regions, where they are heated, to the neighboring colder areas) [38]. These models are most suited for practical three-dimensional simulations, but need as their basis phenomenological constants derived either from experiments or from kinetic modeling.

3.4 Kinetic Models

Kinetic SWP models determine the stationary EEDF $f(\boldsymbol{v}, \boldsymbol{r})$ from the stationary Boltzmann kinetic equation (1). As the anisotropic part of the EEDF is small, a two-term spherical harmonics approximation $f(\boldsymbol{v}, \boldsymbol{r}) = f_0(v, \boldsymbol{r}) + f_1(v, z)\cos(\theta)$ is sufficient, where θ is the angle between the electron velocity vector $\boldsymbol{v}$ and the electric field [here supposed to be applied along the z axis so that $\boldsymbol{E} = (0, 0, E)$]. The small anisotropic part f_1 can be expressed in terms f_0 and the problem is reduced to computing only the isotropic part $f_0(v, \boldsymbol{r})$. The zero momentum of f_0 gives the electron density $n_e(\boldsymbol{r})$ at all points in the discharge, and $n_e(\boldsymbol{r})$ determines the local plasma permittivity [simplest expression $\varepsilon_p = 1 - (n_e/n_c)/(1 + i\nu/\omega)$] entering Maxwell equations. The latter govern the microwave intensity profile $\tilde{\boldsymbol{E}}(\boldsymbol{r})$ necessary for the electron Boltzmann kinetic equation (1). Therefore the EEDF and the microwave electromagnetic fields have to be found by solving Maxwell and Boltzmann equations simultaneously in a self-consistent way. The quasi-neutrality, the Bohm criterion, and the expressions for the ion diffusion and the ionization rate close the model.

The kinetic models occupy an intermediate position between the fluid and particle dynamic simulations: some kinetic information is included and found self-consistently in much more details than in the fluid models (not only temperatures or average energies, but energy distributions), but the movements of the individual particles are not traced. This approach makes sense. Indeed, even if we had information about all individual particle movements, anyway we would have to average this information at the end in order to present it in understandable form. Hence the advantage of PIC-MCC methods is not so much in the detailed information provided (anyway it is averaged at the end), but in the straightforward programming (at the cost of long computation times). Programming for kinetic models is not so easy, but the economy of computation time pays for the effort.

There are two major groups of kinetic SWP models: local and non-local. The classification is based on the ratio of the electron relaxation length λ_ε to the characteristic size of the field inhomogeneity L. The electron relaxation length is estimated as $\lambda_\varepsilon \approx (\lambda\lambda^*/3)^{1/2}$ from the mean free-paths for eleastic and inelastic collisions (λ and λ^*, respectively) in the EEDF tail. The local kinetic models are used for higher pressures, where $\lambda_\varepsilon \ll L$, and the EEDF $f_0(v, \boldsymbol{r})$ at any position $\boldsymbol{r}$ in the discharge is governed by the local electric field intensity $\tilde{\boldsymbol{E}}(\boldsymbol{r})$ there [39].

Non-local models are used in the opposite case of low pressures, for which $\lambda_\varepsilon \gg L$ ([40,41]). For such conditions most of the time the electron does not experience non-elastic collisions and drifts via elastic collisions in the plasma potential well $e\Phi(\boldsymbol{r})$ preserving its total energy $\varepsilon = e\Phi(\boldsymbol{r}) + m_e\boldsymbol{v}^2/2$ or eventually slowly changing it via accumulation of small interactions with the oscillating field $\tilde{\boldsymbol{E}}(\boldsymbol{r})$. Boltzmann equation (1) with the two-term spherical harmonics approximation describes the electron flux in the 4 dimensional $(v, \boldsymbol{r})$ space with the first and second terms corresponding to fluxes in space and along the forth dimension (the velocity axis), respectively. Changing the independent variables in (1)

from (v, $\boldsymbol{r}$) to (ε, $\boldsymbol{r}$) via the transformation $\varepsilon = e\Phi(\boldsymbol{r}) + m_e\boldsymbol{v}^2/2$ and introducing explicit notation for the space and energy fluxes $\boldsymbol{J}_r$ and $\boldsymbol{J}_\varepsilon$, Boltzmann equation is brought to the form

$$\nabla_{\boldsymbol{r}}\cdot\boldsymbol{J}_r + \frac{\partial J_\varepsilon}{\partial\varepsilon} = \nu S^*(f_0) = \nu\sum_k\left[-\nu_k^*(u)\,f_0(\varepsilon,\boldsymbol{r}) + \frac{v_k}{v}\nu_k^*(u+\varepsilon_k)\,f_0(\varepsilon+\varepsilon_k,\boldsymbol{r})\right]. \quad (2)$$

Here the inelastic collision integral on the right-hand side is explicitly written down in terms of the inelastic collision frequencies $\nu_k^*(u)$ and the respective threshold energies ε_k, $u = m_e\boldsymbol{v}^2/2 = \varepsilon - e\Phi$ is the electron kinetic energy, and v_k is the electron velocity corresponding to kinetic energy $u + \varepsilon_k$. The contribution of elastic collisions with the heavy background neutral particles of mass M can be neglected (as done in eq. 2) because it is proportional to $m_e/M \ll 1$. Electron-electron collisions can be added, too.

In the new variables (ε, $\boldsymbol{r}$) the explicit dependence of $f_0(\varepsilon, \boldsymbol{r})$ on $\boldsymbol{r}$ is very weak (negligible) as a result of the slow energy relaxation, because the electron traverses the plasma volume many times before any significant change of its total energy occurs. Therefore the EEDF $f_0(\varepsilon)$ becomes a function of a single variable: the total electron energy $\varepsilon = e\Phi(\boldsymbol{r}) + m_e\boldsymbol{v}^2/2$. The EEDF still depends on $\boldsymbol{r}$, but only indirectly via the plasma potential $\Phi(\boldsymbol{r})$ encapsulated in ε. One can take advantage of this simplification to average (2) over the volume $V(\varepsilon)$ available to electrons of total energy ε. Thus one obtains the space-averaged kinetic equation in the form:

$$\frac{\mathrm{d}}{\mathrm{d}\varepsilon}\,\overline{\nu D_\varepsilon(\varepsilon)}\,\frac{\mathrm{d}f_0(\varepsilon)}{\mathrm{d}\varepsilon} = \overline{\nu\cdot\nu^*(\varepsilon)}\,f_0, \quad (3)$$

where the overbar indicates averaging over $V(\varepsilon)$ and the right-hand side is a short notation for the averaged right-hand side of (2). The averaging volume $V(\varepsilon)$ is limited by the "turning-point surface" $S(\varepsilon)$ where $\varepsilon = e\Phi(\boldsymbol{r})$ and the electron kinetic energy vanishes. Eq. (3) describes the balance of the two processes that can change the total electron energy: accumulation of small energy gains/losses via acceleration/deceleration by the oscillating field $\tilde{\boldsymbol{E}}(\boldsymbol{r})$ and sudden energy losses by inelastic collisions (including the birth of new free electrons via ionization and the loss of high-energy electrons hitting the wall). The space-averaged kinetic equation (3) is an ordinary differential equation for $f_0(\varepsilon)$ with a single independent variable ε. Such a simple form (3) resulted because, first, $\boldsymbol{J}_r(\varepsilon)$ vanishes along the boundary $S(\varepsilon)$ (where $v = 0$) and, therefore, the first term of (2) disappears after integrating over $V(\varepsilon)$. Strictly speaking, this is not true for electrons with energy higher than the wall potential, but it can be dealt with by introducing an additional "wall collision term" in the inelastic collisions integral. The second helpful circumstance was the absence of explicit dependence of $f_0(\varepsilon)$ on $\boldsymbol{r}$. This permitted factoring out $f_0(\varepsilon)$ in the averaging. If the explicit $\boldsymbol{r}$ dependence $f_0(\varepsilon, \boldsymbol{r})$ were preserved, the averaging in (3) would have had to extend over $f_0(\varepsilon, \boldsymbol{r})$ and the resulting space-averaged equation would have been of limited (if any) usefulness.

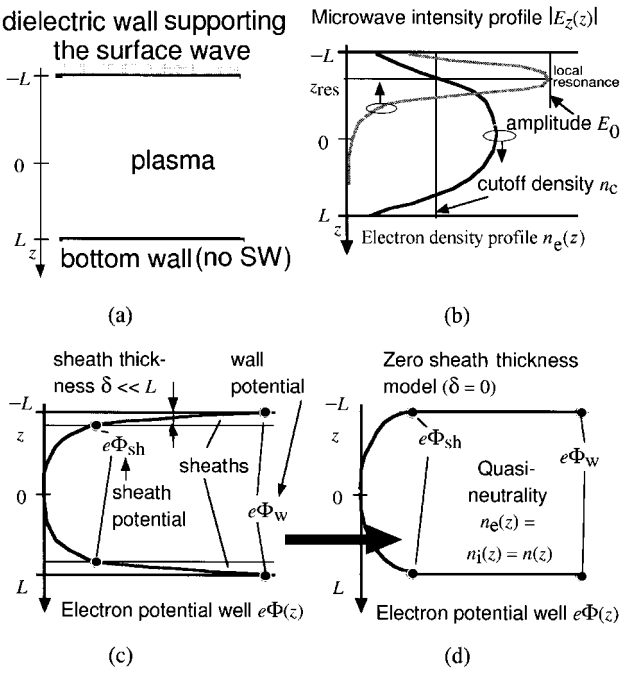

Fig. 1 One dimensional SW plasma model.

The space-averaged kinetic equation (3) corresponds to one-dimensional diffusion of the electrons in the energy space along the total energy (ε) axis with energy-dependent diffusion coefficient $D_\varepsilon(\varepsilon)$ (not to be confused with the space diffusion coefficient D) and source and sink terms on the right-hand side related to non-elastic processes. Such diffusion, as any diffusion, can be regarded as a sequence of random steps (in our case random energy gains/losses or steps $\Delta\varepsilon$ along the energy axis ε) occurring with average frequency ν_ε, and the corresponding diffusion coefficient can be expressed via the average length and frequency of such steps as $D_\varepsilon = (\Delta\varepsilon)^2\nu_\varepsilon/3$. Both $\Delta\varepsilon$ and ν_ε can be and usually are energy dependent, and the particular form of $D_\varepsilon(\varepsilon)$ results from the spatial distribution and temporal dependence of the oscillating electric field $\tilde{\boldsymbol{E}}(\boldsymbol{r}, t)$.

The non-local approach has been successfully applied to SWP simulation [42-44]. Let us demonstrate the kinetic SWP simulation on the example of a one-dimensional non-local SW model with non-collisional heating at the plasma electron resonance [43,44]. The plasma of neutral density n_n and thickness $2L$ is sustained between two parallel walls and is considered homogeneous along x and y (Fig. 1(a)). The energy $e\Phi(z) > 0$ of an electron of charge $e = -|e| < 0$ located in the static field of the plasma potential $\Phi(z) < 0$ is treated as a continuous potential well $e\Phi(z)$ in the bulk plasma (increasing gradually from 0 at $z = 0$ to $e\Phi_{sh}$ at the sheath boundary), followed by a discontinuous potential jump from $e\Phi_{sh}$ to $e\Phi_w$ in the sheath (Fig. 1(c)). The sheath is treated as an infinitely thin double layer (Fig. 1(d)) and the detailed density profiles in the sheaths are not sought. The dielectric-plasma interface with the SW excitation is along

the $z = -L$ wall. Although the excitation is asymmetric, the electron density profile is symmetric in respect to $z = 0$ due to the very fast spatial diffusion of the electrons, which removes the influence of the asymmetric electron heating (Fig. 1(b)). We suppose that at the center the electron density n_e is higher than the cut-off density n_c (overdense plasma) but lower than n_c near the walls. Thus resonance conditions ($n_e = n_c$) occur at some position $z = z_{res}$ (Fig. 1(b)). In this case the space averaging in (3) is performed over the z interval for which $e\Phi(z) < \varepsilon$, i.e. the interval between the two roots of the equation $e\Phi(z) = \varepsilon$. Solving the space-averaged kinetic equation (3) requires knowledge of the plasma potential profile $\Phi(z)$.

For low pressures the collisional electron heating can be neglected, and the diffusion (in energy space) occurs by frequent small random energy gains/losses $\Delta\varepsilon$ when the electrons pass through the electron plasma resonance around $z = z_{res}$. The "energy-kick frequency" ν_ε is determined by the average time between two consecutive passages of the electron through the resonance zone. Each individual step can with the same probability result in electron energy gain or loss, but we get total energy gain (electron heating) because the electron flux from the body to the tail of the EEDF prevails over the opposite flux from the tail to the body. This is simply due to the fact that there are more electrons in the body than in the tail of the EEDF.

In order to compute the energy gain/loss $\Delta\varepsilon$ for a single passage through the resonance we need some knowledge about the oscillating electric field $\tilde{\boldsymbol{E}}(\boldsymbol{r}, t)$. Only the profile near the resonance is necessary because far from it the fields are, first, much weaker, and, second, too homogeneous to cause non-collisional transit-time heating (homogeneous non-resonant oscillating fields cannot heat the electrons without the help of collisions: in each individual oscillation the amounts of energy gained and lost by the electron by acceleration/deceleration cancel out). Near the resonance the electric field component along the density gradient (E_z) is much stronger than all other components, so that one can neglect E_x and E_y. The remaining component E_z can be obtained for the TM mode (wave components E_z, E_y, H_x) from Maxwell equations. We approximate the electron density near the resonance as $n_e(z) = n_c + (dn_e/dz)\,\Delta z$, where $\Delta z = z - z_{res}$ is the distance from the resonance. Then the plasma permittivity can be written as

$$\begin{aligned}\varepsilon_p(z) &\approx 1 - [n_e(z)/n_c] + i\,(\nu/\omega)\,[n_e(z)/n_c] \\ &= i\,(\nu/\omega)\,(1 + i\,\Delta z/\Delta)\,, \end{aligned} \tag{4}$$

where

$$\Delta = \frac{\nu}{\omega}\frac{n_e}{dn_e/dz} \tag{5}$$

is the width of the resonance, and $\nu \ll \omega$ is assumed. From Maxwell equations $E_z = [i/\omega\varepsilon_0\varepsilon_p(z)](\partial H_x/\partial y)$. $\partial H_x/\partial y$ varies only slowly over the resonance width Δz and can be considered constant there. Therefore, introducing the approximation (4) for $\varepsilon_p(z)$, one gets the relation between profiles of electron density and oscillating electric field amplitude in the form [13]

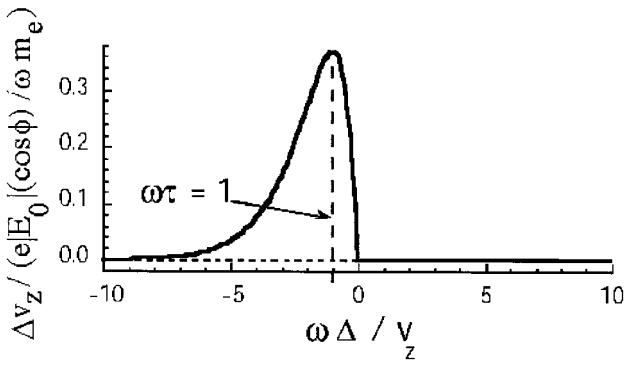

Fig. 2 Dependence of the electron velocity "kick" (8) on v_z; $t = D/|v_z|$ is the electron transit time.

$$E_z(z,t) = \mathrm{Re}\left(\frac{E_0\, e^{-i\omega t}}{1 + i\Delta z/\Delta}\right), \tag{6}$$

where E_0 stays for the presumably constant $E_0 = (1/\nu\varepsilon_0)(\partial H_x/\partial y)$. For very low pressures (including the example we give below) the transport electron-neutral collision frequency ν in (5) has to be replaced by the electron thermal convection frequency $\nu_{conv} = \omega(\nu_{th}/\omega)^{2/3}\,(n_c/|dn_e/dz|)^{-2/3}$ [45], if $\nu_{conv} > \nu$.

It is interesting to note that electrons passing through the resonance (6) in direction along the density gradient (from the wall to the bulk) are *not* affected in first approximation. Indeed, let us compute the velocity change Δv_z of an electron passing trough the resonance field (6)

$$\Delta v_z = \frac{e}{m_e}\int_{-\infty}^{+\infty} E_z\left[z(t), t\right] dt \tag{7}$$

assuming that the velocity "kick" is small ($|\Delta v_z| \ll |v_z|$), so that one can approximate the electron position $z(t)$ in (7) as $z(t) = z_{res} + v_z\, t$ ($t = 0$ is chosen to be the moment when the electron passes through $z = z_{res}$). The result is (Fig. 2)

$$\Delta v_z = \begin{cases} 0, & \text{for } v_z > 0 \\ 2\pi\,\dfrac{e}{m_e}\,|E_0|\,(\cos\varphi)\,\tau e^{-\omega\tau}, & \text{otherwise}, \end{cases} \tag{8}$$

where $\tau = \Delta/|v_z|$ is the electron transit time and φ is the phase of the oscillating electric field at $t = 0$ (the moment when the electron passes through $z = z_{res}$). This strange result can be easily understood, if we consider the resonance field (6) as superposition of plane waves $e^{i(k_z z - \omega t)}$ and obtain the complex amplitudes of all such partial waves by inverse Fourier transform of (6). All amplitudes for $k_z > 0$ turn out to be zero, while all amplitudes for $k_z < 0$ are non-zero with a maximal amplitude for $k_z = -1/\Delta$. Thus, (6) is a superposition only of waves traveling from the plasma bulk to the walls. For any

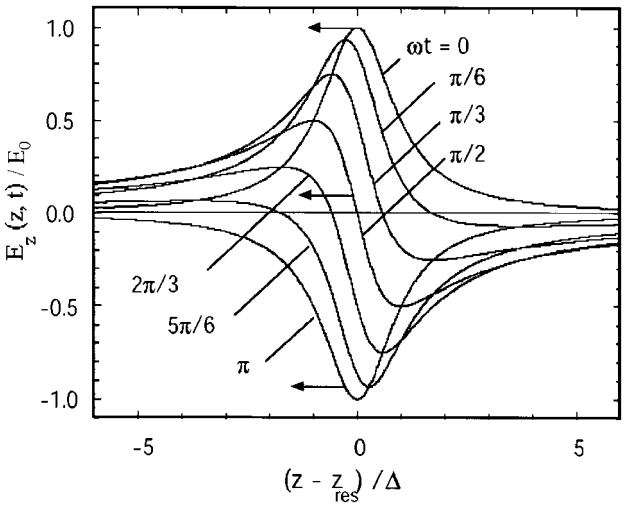

Fig. 3 Time evolution of the microwave electric field in the resonance for half a time period.

electron running to the wall some of the partial waves will have close phase velocities and will have accelerating or decelerating effect depending on the phase φ. The most effective interaction will be for electrons synchronous with the highest-amplitude wave, i.e. for $k_z = -1/\Delta$, or phase and electron velocity $v_{ph} = \omega/k_z = -\omega\Delta$. The transit time for such electrons is $\tau = 1/\omega$, which corresponds to the maximum of (8) at $\omega\tau = 1$. For electrons running in the opposite direction there are no synchronous partial waves and thus no interaction. The "traveling wave" nature of the resonance field (6) is demonstrated directly in Fig. 3 by plotting the time evolution for half time period.

To determine the position and width of the resonance in (6) we need the electron density profile. It is easily derived from the EEDF $f_0(\varepsilon)$ and the plasma potential profile $\Phi(z)$ via integration over the electron kinetic energy $u = m_e \boldsymbol{v}^2/2$:

$$n_e(z) = n_e[\Phi(z)] = 2\pi\left(\frac{2}{m_e}\right)^{\frac{3}{2}} \int_{-\infty}^{+\infty} f_0[u + e\Phi(z)]\, u^{1/2}\, du. \qquad (9)$$

The plasma potential profile $\Phi(z)$ is necessary at various steps of the simulation: for computing the electron density profile from (9), for determining the area of averaging in eq. (3), for computing the spatially dependent kinetic energy $u(z) = \varepsilon - e\Phi(z)$ to be used with various collision cross-sections, which depend on u and not on the total energy ε [see e.g. the ionization cross-section σ_i in eq. (11) below]. The modeling can be based on some initial estimate for $\Phi(z)$, but ultimately we want to get $\Phi(z)$ in a self-consistent manner. This is achieved making use of the quasi-neutrality $n_e = n_i = n$ and of the ion balance between ionization and ion drift down the plasma potential gradient

$$\frac{d}{dz} v_{id}(z)\, n[\Phi(z)] = I[\Phi(z)]\ ,$$
$$v_{id}(z) = -\, b_{id} \frac{d}{dz}\Phi(z)\ ,\ n = n_i = n_e\ . \qquad (10)$$

Here v_{id} and b_{id} are the ion drift velocity and mobility, respectively, and the dependence (9) of the plasma density n on the local plasma potential $\Phi(z)$ and the similar dependence of the ionization rate

$$I(z) = I[\Phi(z)] = 2\pi\left(\frac{2}{m_e}\right)^2 n_n \int_0^{+\infty} \sigma_i(u)\, f_0[u + e\Phi(z)]\, u\ du \qquad (11)$$

have been introduced explicitly in the notation. For a known EEDF $f_0(\varepsilon)$ eqs. (9–11) give a set of two first order ordinary differential equations for the two unknown functions $\Phi(z)$ and $v_{id}(z)$, that are readily solved numerically. The natural boundary conditions are $\Phi(z = 0) = 0$ and $v_{id}(z = 0) = 0$.

In addition to providing the plasma density profile $\Phi(z)$ needed as described above, this gives also the ion drift velocity $v_{id}(\pm L)$ of the ions entering the sheath regions. This velocity must be equal to the Bohm velocity, but nothing in the procedure described to this point made any use of it. This provides a tool to determine the microwave intensity E_0 of the applied microwave field in a self-consistent way: E_0 is adjusted until the Bohm criterion is satisfied. This works because any change of E_0 changes the "kicks" Δv_z and $\Delta\varepsilon$ of electron velocity and energy, and via them - the energy diffusion coefficient D_ε entering the space-averaged kinetic equation (3). The resulting new EEDF results in new ionization rate (11) and shifts the value of $v_{id}(\pm L)$ one or the other way until it eventually becomes equal to the Bohm velocity. The value of E_0 for which this happens gives the self-consistent solution.

The last quantity which needs to be determined self-consistently is the wall potential Φ_w (for definition recall Fig. 1(d)). This can be done from the balance of total ionization in the entire plasma volume $\int_{-L}^{+L} I(z)\, dz$ and the electron loss at the walls, since the latter depends on the wall potential. Indeed, all electrons that reach the sheath boundary with $|v_z|$ higher than $\sqrt{2|e|(\Phi_w - \Phi_{sh})/m_e}$ will be lost after hitting the wall. Thus the wall potential Φ_w is self-consistently adjusted to keep the number of the lost electrons equal to the number of electrons created by ionization in the plasma volume.

All these relations make it possible to compute numerically in a self-consistent way the EEDF, the plasma potential profile (including the wall potential Φ_w) and the microwave intensity profile, starting from a limited set of input parameters. The most natural choice is to start from the gas pressure and temperature, the size of the structure ($2L$) and the frequency and intensity of the externally applied microwave field (in our case characterized by the amplitude in the resonance E_0). Once the EEDF and the potential profile are found, all other quantities of interest are derived from (4–11). Computationally, it is more convenient to start from the plasma size $2L$, the neutral density n_n, and the position of the resonance z_{res} (this defines one point in the electron density profile) and to compute the self consistent microwave field E_0 necessary to bring the resonance to that point, finding on the way the self-consistent EEDF, plasma potential and all

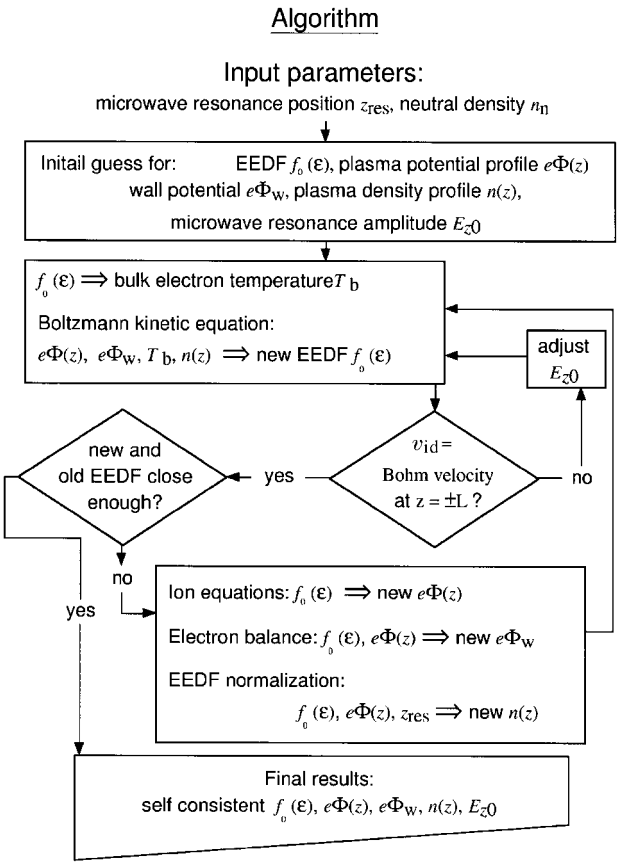

Fig. 4 Numerical algorithm.

derived quantities like electron density and ionization rate profiles (9) and (11). The iterative flow-chart is shown in Fig. 4. The first step of the iteration needs some initial estimates, which are further improved until we are satisfied with the "closeness" of the successive solutions.

Figures 5, 6 and 7 show an example of a self-consistent solution for 20 mTorr 300 K ($n_n = 6 \times 10^{14}$ cm^{-3}) argon microwave ($\omega/2\pi = 817$ MHz) plasma of size $L = 24$ cm for resonance position z_{res} set at 7 mm from the wall. The non-local character of the discharge is clearly visible from Fig. 7: the ionization rate profile is totally unrelated to the microwave intensity profile. The bi-Maxwellian EEDF results from the selective heating only of electrons with energy higher than the resonance potential energy $e\Phi(z_{res}) \approx 3.5$ eV. Electrons with lower energies are not directly affected by the microwave field, since they cannot reach the resonance region. Such electrons can gain energy only via electron-electron collisions, which has Maxwellizing effect.

3.5 Conclusion

The results from the 1d kinetic model are in good qualitative agreement with the experiment. Indeed, measurements by Sugai *et al.* [46] clearly confirm the bi-Maxwellian EEDF as predicted from Fig. 5, while the electron density and microwave intensity profiles reported in [16] convincingly show a local resonance occurring at $n_e = n_c$, as

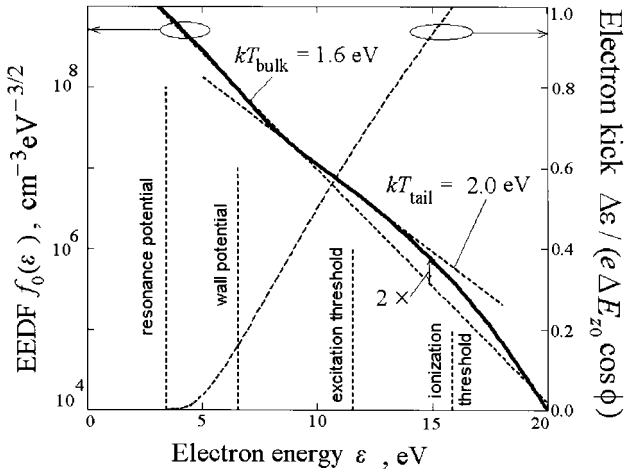

Fig. 5 The self consistent EEDF and the electron kick from the resonance.

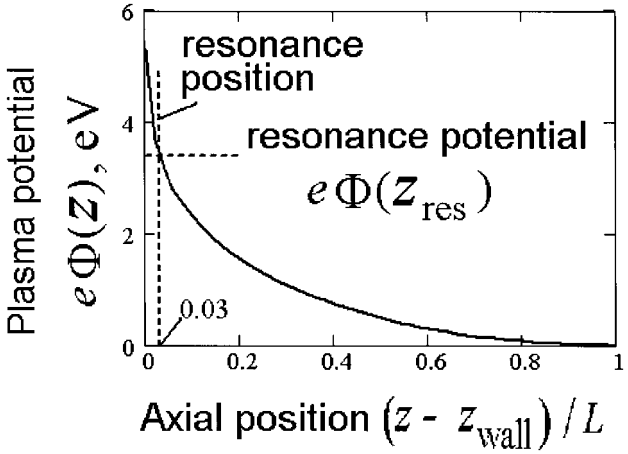

Fig. 6 Self-consistent plasma potential.

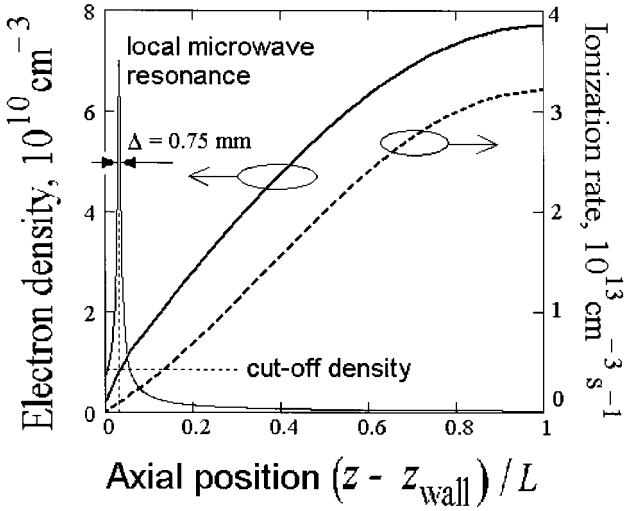

Fig. 7 Self-consistent profiles of electron density, ionization rate and microwave intensity.

predicted in Fig. 7. Space resolved electron temperature measurements [47] support the direction of the electron kick to the wall, as predicted by eq. (8): rather high electron temperatures are observed very close to the wall, but not in the bulk of the plasma, although the distance between the hot and cold regions is much less than the electron free path for the applicable pressure. This can be explained by the accelerated electrons hitting the walls without reaching the plasma bulk and would not occur if the electrons were accelerated randomly in all directions in the resonance region.

References

[1] A.W. Trivelpiece and R.W. Gould, J. Appl. Phys. **30**, 1784 (1959).

[2] A.W. Trivelpiece, *Slow Wave Propagation in Plasma Waveguides* (San Francisco Press, 1967).

[3] M. Moisan, C. Baudry and P. Leprince, IEEE Trans. Plasma Sci. **PS-3**, 55 (1975).

[4] M. Moisan, C. Baudry, L. Bertrand, E. Bloyet, J.M. Gagnè, P. Leprince, J. Marec, G. Mitchel, A. Ricard and Z. Zakrzewski, in *Gas Discharges* (*IEE Conference Publication*, **143**, 1976) p. 382.

[5] K. Komachi and S. Kobayashi, J. Microwave Power Electromagn. Energy **24**, 140 (1989).

[6] M. Nagatsu, G. Xu, I. Ghanashev, M. Kanoh and H. Sugai, *Proc. 13th Symposium on Plasma Processing, Tokyo, 29–31 Jan. 1996*, ed. T. Makabe (Tokyo, Japan Society of Applied Physics, 1996) p. 9.

[7] H. Sugai, I. Ghanashev and M. Nagatsu, Plasma Sources Sci. Technol. **7**, 192 (1998).

[8] M. Nagatsu, I. Ghanashev and H. Sugai, Plasma Sources Sci. Technol. **7**, 230 (1998).

[9] I.P. Ganachev and H. Sugai, Plasma Sources Sci. Technol. **11**, A178 (2002).

[10] I. Ganachev and H. Sugai, Sur. Coatings Technol. **174-175**, 15 (2003).

[11] E. Fermi, Phys. Rev. **75**, 1169 (1949).

[12] M.M. Turner, Phys. Rev. Let. **71**, 1844 (1993).

[13] V.L. Ginzburg, *The Propagation of Electromagnetic Waves in Plasmas* (Pergamon, Oxford, 1964) p. 227.

[14] K.N. Stepanov, Zh. Tekh. Fiz. **35**, 1002 (1965); translation, Sov. Phys. – Techn. Phys. **10**, 773 (1965).

[15] M. Zethoff and U. Kortshagen, J. Phys. D: Appl. Phys. **25**, 1574 (1992).

[16] I. Ghanashev, H. Sugai, S. Morita and N. Toyoda, Plasma Sources Sci. Technol. **8**, 363 (1999).

[17] A.I. Akhiezer and A.S. Bakai, Sov. Phys. Doklady **16**, 1065 (1972).

[18] O. Buneman, Phys. Rev. **115**, 503 (1959).

[19] J.M. Dawson, Phys. Rev. **118**, 381 (1960).

[20] C.K. Birdsall and A.B. Langdon, *Plasma Physics via Computer Simulation* (IOP Publishing, Bristol, 1991).

[21] 卜部友二, 小見山分行, 子越澄雄：電気学会研究会資料 (Papers of the Technical Meeting on Plasma Science and Technology, IEE Japan) **PST-02** (2002) 43.

[22] A. Katamoto, Y. Urabe, S. Kogoshi and K. Fujisaki, *Proc. Joint Conf. Of ESCAMPIG 16 and ICRP 5*, (2002) Vol.1, p. 253.

[23] S. Kogoshi, *Microwave Plasma Engineering* (*Maikuroha Purazuma-no Gijutu*), ed. H. Sugai (Ohmsha, Tokyo, 2003), sec. 4.2 (in Japanese).

[24] I. Ghanashev, M. Nagatsu and H. Sugai, Jpn. J. Appl. Phys. **36**, 337 (1997).

[25] M. Walter, D. Korzec, M. Hütten and J. Engemann, Jpn. J. Appl. Phys. **36**, 4777 (1997).

[26] Y. Yasaka, D. Nozaki, K. Koga, M. Ando, T. Yamamoto, N. Goto, N. Shii and T. Morimoto, Jpn. J. Appl. Phys. **38**, 4309 (1999).

[27] 桂井　誠：電学論 A, **120**, 5, 583 (2000).

[28] Y. Yasaka and H. Hojo, Phys. Plasmas **7**, 1601 (2000).

[29] V.M.M. Glaude, M. Moisan, R. Pantel, P. Leprince and J. Marec, J. Appl. Phys. **51**, 5693 (1980).

[30] E. Mateev and I. Zhelyazkov, J. Appl. Phys. **54**, 3049 (1983).

[31] J. Margot and M. Moisan, J. Plasma Phys. **49**, 357 (1993).

[32] I. Ghanashev, M. Nagatsu, G. Xu and H. Sugai, Jpn. J. Appl. Phys. **36**, 4704 (1997).

[33] I. Ghanashev and H. Sugai, Phys. Plasmas **7**, 3051 (2000).

[34] C.M. Ferreira, J. Phys. D: Appl. Phys. **16**, 1673 (1983).

[35] A.B. Sá and C.M. Ferreira, J. Appl. Phys. **70**, 4147 (1991).

[36] I. Odrobina and M. Kando, 信学技報 (Technical Report of IEICE Japan) **SDM96-110** (1996) p. 23.

[37] I. Odrobina and M. Kando, *Proc. 1996 Int. Conf. on Plasma Physics* (Nagoya, 1996) p. 1366.

[38] T. Toba and M. Katsurai, IEEE Trans. Plasma Sci. **30**, 2095 (2002).

[39] M. Ferreira and J. Loureiro, J. Phys. D: Appl. Phys **16**, 2471 (1983).

[40] I.B. Bernstein and T. Holstein, Phys. Rev. **94**, 1475 (1954).

[41] L.D. Tsendin, Zh. Eksp. Teor. Fiz. **66**, 1638 (1974); translation Sov. Phys.-JETP **39**, 805 (1974).

[42] U. Kortshagen, J. Phys. D: Appl. Phys. **26**, 1691 (1993).

[43] I. Ghanashev, L. Tsendin and H. Sugai, *4th Int. Workshop Microwave Discharges: Fundamentals and Applications*, Zvenigorod, Russia, 18–22 Sep. 2000, p. 26.

[44] I. Ganachev, L.D. Tsendin and H. Sugai, *Proceedings of the Joint 16th ESCAMPIG and 5th ICRP*, Grenoble, France, July 14–18, 2002, eds. N. Sadeghi and H. Sugai, Vol. 1, p. 217.

[45] Yu. M. Aliev, Y. Yu. Bychenkov, A.V. Maximov and H. Schlüter, Plasma Sources Sci. Technol. **1**, 126 (1992).

[46] H. Sugai, I. Ghanashev, M. Hosokawa, K. Mizuno, K. Nakamura, H. Toyoda and K. Yamauchi, Plasma Sources Sci. Technol. **10**, 378 (2001).

[47] M. Nagatsu, T. Niwa and H. Sugai, Appl. Phys. Lett. **81**, 1966 (2002).